JACS
JOURNAL OF THE AMERICAN CHEMICAL SOCIETY
Article
pubs.acs.org/JACS

Platinum Metal-Free Catalysts for Selective Soft Oxidative Methane → Ethylene Coupling. Scope and Mechanistic Observations

Matthias Peter and Tobin J. Marks*

Department of Chemistry and the Center for Catalysis and Surface Science, Northwestern University, Evanston, Illinois 60208-3113, United States

Supporting Information

ABSTRACT: Using abundant soft oxidants, a high methane-to-ethylene conversion might be achievable due to the low thermodynamic driving force for over-oxidation. Here we report on the oxidative coupling of methane by gaseous S_2 (SOCM). The catalytic properties of Pd/Fe_3O_4 are compared with those of Fe_3O_4, and it is found that high ethylene selectivities can be achieved without noble metals; conversion and selectivity on Fe_3O_4 are stable for at least 48 h at SOCM conditions. SOCM data for 10 oxides are compared, and ethylene selectivities as high as 33% are found; the C_2H_4/C_2H_6 ratios of 9−12 observed at the highest S_2 conversions are significantly higher than the C_2H_4/C_2H_6 ratios usually found in the CH_4 coupling with O_2. Complementary in-detail analytical studies show that, on Mg, Zr, Sm, W, and La catalysts, which strongly coke during the reaction, lower ethylene selectivities are observed than on Fe, Ti, and Cr catalysts, which only coke to a minor extent. Further catalyst-dependent changes during SOCM in surface area, surface composition, and partial conversion to oxysulfides and sulfides are discussed. Evidence concerning the reaction mechanism is obtained taking into account the selectivity for the different reaction products versus the contact time. CH_4 coupling proceeds non-oxidatively with the evolution of H_2 on some catalysts, and evidence is presented that C_2H_4 and C_2H_2 formation occur via C_2H_6 and C_2H_4 dehydrogenation, respectively.

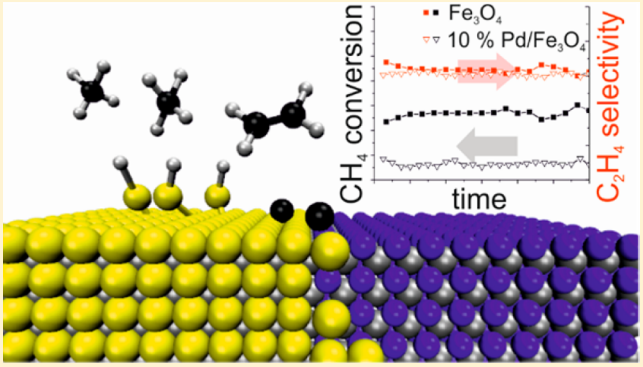

INTRODUCTION

Increasing demands for ethylene as a chemical feedstock along with declining petroleum reserves and the emergence of shale gas have stimulated renewed interest in direct and efficient catalytic processes for the oxidative coupling of methane (OCM) to ethylene.[1] Numerous studies of OCM with O_2 as the oxidant have focused on optimizing C_2 yields[2] and elucidating the reaction mechanism.[3] On alkaline earth oxides and lanthanide oxides, C_2 selectivities and C_2 yields of 50−70% and 8−11%, respectively, have been reported.[3b] The C_2 yields are nearly doubled by adding dopants such as alkali and alkaline earth metals.[3a]

Regardless of the significant advances in this field, industrial applications of OCM remain in their infancy.[4] To a large extent, this can be attributed to the strong thermodynamic driving force for over-oxidation: conversion of the C_2 products to CO_x and other byproducts compromises the C_2 yield. Furthermore, the strong exothermicity of the reaction introduces heat management and reactor design challenges.

The intrinsic instability of many OCM catalysts poses a further complexity.[2h,5] A prominent example is one of the most frequently studied OCM catalysts, Li/MgO. In many early studies, stability tests were not reported, or this catalyst was found to be stable. Recently it has been shown that Li/MgO suffers from an intrinsic instability, which prohibits practical applications.[6] Other approaches for converting CH_4 to valuable hydrocarbon feedstocks, such as the conversion to methanol[7] or formaldehyde[8] or non-oxidative CH_4 coupling,[9] have attractions but also significant limitations and have not seen large-scale use.

A recent approach for CH_4-to-C_2H_4 coupling seeks to moderate the driving force for methane over-oxidation with the "soft" oxidant S_2 ("SOCM").[10] Note that ΔG for CH_4 over-oxidation by S_2 is only −236 kJ/mol, versus −1294 kJ/mol for O_2 (Figure 1), suggesting that higher ethylene selectivities/yields might be possible using less aggressive oxidants in the presence of an appropriate catalyst. The lower SOCM exothermicity versus OCM with O_2 might also offer advantages in reactor design, and the H_2S co-product could be efficiently recycled to S_8 via the efficient Claus process.[11]

The conversion of S_2 with methane was studied extensively between 1927 and the mid 1950s for the commercial production of CS_2,[12] and CS_2 yields are highest at temperatures of 500−700 °C and CH_4/S_2 ratios of ∼1. Early studies on the $CH_4 \rightarrow C_2H_4$ reaction showed that the CH_4 conversions are

Received: September 21, 2015
Published: November 9, 2015

DOI: 10.1021/jacs.5b09939
J. Am. Chem. Soc. 2015, 137, 15234−15240

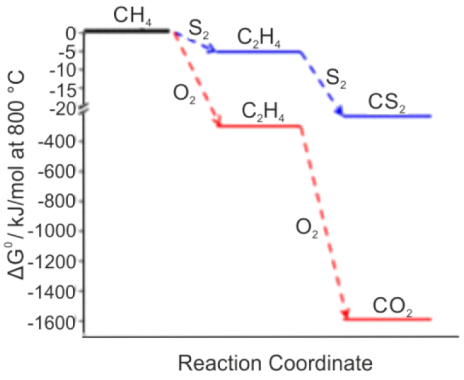

Figure 1. Comparison of the free energies of the principal species involved in the oxidative coupling of CH_4 by S_2 (blue) and O_2 (red) at 800 °C.

<5% at low temperatures, whereas excessive coking takes place at high temperatures.[13] Didenko et al. found a high selectivity to mercaptans, which is in contrast to the other two studies.[14] In our earlier SOCM work on neat metal chalcogenide catalysts (e.g., TiS_2, RuS_2, MoS_2, and PdS), we obtained CH_4 conversions and C_2H_4 selectivities at 950 °C of 6−9% and 4−9%, respectively.[10] Note that no coke was observed under any of the reaction conditions. DFT computation finds that the M−S bond strength has a major influence on SOCM conversion and selectivity, which are inversely related.[6,10] Enhanced catalytic performance was also observed when PdS_x was supported on oxides such as ZrO_2.[10]

These initial findings raise the question as to whether PdS_x shows enhanced activity/selectivity due to the interaction with the support or whether the oxide support by itself may be active in SOCM processes. Furthermore, information on the evolution of catalyst structure/composition under reaction conditions may be pivotal for understanding the catalytic properties. Finally, no experimental data on the SOCM reaction mechanism are available. In particular, since several OCM studies showed that non-oxidative coupling takes place at elevated temperatures, evidence for the relevance of this reaction route during SOCM would be revealing.

To address these questions in the present full account, we first examine the catalytic properties of Pd over iron oxide and over bare iron oxide. Next, in a systematic study of neat oxide-derived catalysts for SOCM, the differences in the catalytic properties of 10 different materials are compared, and information on the SOCM reaction mechanism is provided. Significantly higher C_2H_4 yields and selectivities are achieved than previously found with PdS_x and supported PdS_x. Combining the catalytic measurements with catalyst structural/compositional analysis allows a correlation to be made between catalytic properties and catalyst evolution under reaction conditions.

EXPERIMENTAL SECTION

The 10 oxide nanopowders used in the current experiments were purchased from Sigma-Aldrich, Strem Chemicals, or Alfa Aesar and have stated purities of ≥99.95%. Pd/Fe_3O_4 was prepared by incipient wetness impregnation of Fe_3O_4 with $Pd(NO_3)_2{\cdot}2H_2O$ and subsequent calcination under O_2 at 550 °C for 6 h. Reactor measurements were carried out in the custom packed bed reactor described previously,[10] loaded with 200 mg of precatalyst with a particle size of 180−300 μm in a quartz tube. The packed-bed automated reactor was designed to use S_2 vapor as the hydrocarbon oxidant.[10] Experiments were performed using 2.7% CH_4 in Ar and a CH_4/S ratio of 7.5, with 0.07% H_2S added to diminish coking. After reaching the reaction temperature of 950 °C, the catalysts were exposed for 4 h to 0.28% S_2 and 0.33% H_2S before exposure to the reaction mixture. After 6 h at a weight hourly space velocity (WHSV = CH_4 mass flow/catalyst mass, scaling as inverse contact time) of 0.785 h^{-1}, the WHSV was decreased to 0.628 h^{-1} for 5 h, and then after 5 h to 0.471 h^{-1} for 5 h. The effluent distribution was continuously monitored by gas chromatography (Agilent 7890A, equipped with FID, TCD, and FPD detector). The activity data reported here are the average of at least three independent measurement sets.

X-ray diffraction (XRD) data on the catalysts after reaction at 950 °C were collected using a powder X-ray diffractometer (Rigaku Ultima IV) with Cu Kα radiation and a Ni filter. The XRD instrument was operated at 40 kV and 20 mA. The step size was set to 0.05° with a count time of 2−3 s per step. A Thermo Scientific ESCALAB 250Xi was employed for the X-ray photoelectron spectroscopy (XPS) experiments. Measurements were conducted with an Al Kα radiation (1486.6 eV) excitation source, an electron flood gun, and a scanning ion gun. On selected catalysts, Raman spectroscopy was performed after reaction at 950 °C under the conditions described above (Acton TriVista CRS, 514.5 nm radiation, 0.2 mW laser power, 5 min collection time). External lab services were employed for the BET surface area measurements and combustion analysis.

RESULTS

Catalytic SOCM studies were carried out under the aforementioned conditions. Figure 2 compares the CH_4

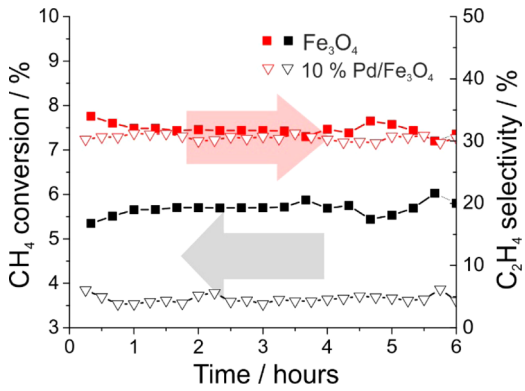

Figure 2. SOCM CH_4 conversion (black) and C_2H_4 selectivity (red) compared on 10 wt% Pd/Fe_3O_4 (triangles) and on Fe_3O_4 (squares) at 950 °C with WHSV = 0.785 h^{-1} and CH_4/S = 7.5.

conversion and C_2H_4 selectivity of 10 wt% Pd/Fe_3O_4 and Fe_3O_4 at WHSV = 0.785 h^{-1}. The obtained C_2H_4 selectivities of >30% are higher by >33% versus previous results on Pd/ZrO_2.[10] The CH_4 conversion is somewhat lower under the present conditions but note that significantly lower temperatures are used here, which were previously shown to afford both lower conversions and C_2H_4 selectivities. The C_2H_4 selectivity of 30−35% is quite similar over Fe_3O_4 and Pd/Fe_3O_4, whereas the CH_4 conversion is slightly lower over Pd/Fe_3O_4. Noble metals are thus clearly unnecessary for high SOCM selectivity to ethylene.

These findings inspired us to study a number of different oxides as catalysts for SOCM. The reaction products invariably consist of C_2H_4, C_2H_6, C_2H_2, and CS_2, with formation of mercaptans, propane, propylene, and propyne <1%. Depending on the catalyst, the C_2H_4/C_2H_6 ratio is in the range 8.9−12.4, with the C_2H_4/C_2H_2 ratio in the range 7.3−16.6 for the lowest WHSV = 0.471 h^{-1}. Importantly, ethylene is by far the most abundant C_2 product, in contrast to typical OCM reactions

DOI: 10.1021/jacs.5b09939
J. Am. Chem. Soc. 2015, 137, 15234−15240

with O_2.[3c,d,15] Figure 3 compares the CH_4 conversions and the C_2H_4 selectivities of 10 oxides after 0, 2, and 6 h on stream with

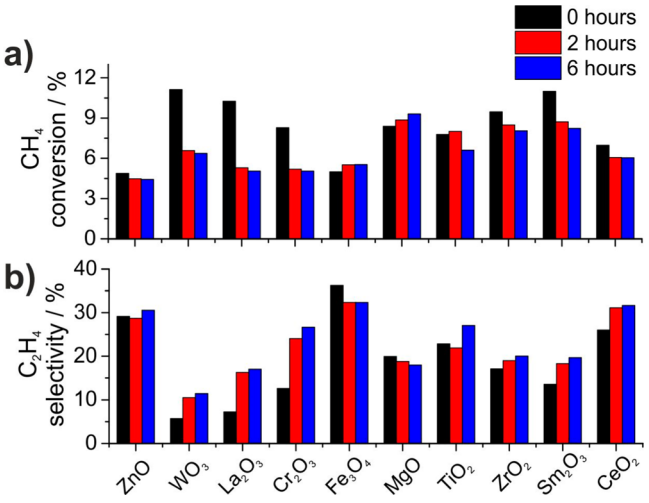

Figure 3. SOCM (a) CH_4 conversion and (b) C_2H_4 selectivity at time = 0 (black), after 2 h (red), and after 6 h (blue) at 950 °C with WHSV = 0.785 h^{-1} and CH_4/S = 7.5.

WHSV = 0.785 at 950 °C. After 6 h, the CH_4 conversions are in the range 4.4−9.3%, whereas the C_2H_4 selectivities are 11.4−30.5%. It can be seen that the variations in CH_4 conversion are relatively small. SOCM at enhanced contact times leads to an even smaller discrepancy between the total CH_4 conversions on the different catalysts; at WHSV = 0.471 h^{-1}, the CH_4 conversions are in the range 7.73−12.05%, whereas the C_2H_4 selectivities are in the range 9.58−25.93%. This observation can be associated with the large S_2 conversion, which is 45−60% for WHSV = 0.785 h^{-1} and >80% for WHSV = 0.471 h^{-1}. It is reasonable to propose that as the reaction mixture passes through the catalyst bed, the reaction rate is initially high and decays as the S_2 concentration decreases. Due to the high total S_2 conversion over all catalysts, only this second stage of lower reaction rate occurs to a different extent over the different catalysts. Accordingly, small variations in the total CH_4 conversions are expected and more so for the lower WHSV due to the corresponding higher S_2 conversion, in agreement with experimental observations.

In contrast to CH_4 conversion, the C_2H_4 selectivities are strongly catalyst dependent, showing that the reaction is highly sensitive to the nature of the catalyst. As evident from Figure 3, both CH_4 conversion and C_2H_4 selectivity change during an initial induction period of ∼2 h after which they remain relatively constant. Stronger variations in the catalytic properties are observed on WO_3, La_2O_3, and Cr_2O_3. On the Zn, Fe, Ce, and Fe catalysts, the C_2H_4 selectivities are greater than 30%, with Fe_3O_4 providing the highest C_2H_4 selectivity of 33%. Conversion and selectivity vs time on stream are summarized in the Supporting Information (SI), page S2. To validate that the catalysts do not deactivate with time, which has been previously found for many OCM catalysts,[2h,5a] the reaction was carried out over Fe_3O_4 for 48 h on stream at WHSV = 0.628 h^{-1} (SI, page S4): CH_4 conversion and C_2H_4 selectivity are stable at 4−5% and ∼30%, respectively.

Note that the C_2H_4 yield increases with decreasing WHSV: it is on average higher by 5% and 6% if the WHSV is decreased from 0.785 h^{-1} to 0.628 h^{-1} and further to 0.471 h^{-1}, respectively. In contrast to these results, SOCM over the noble metal catalysts reported earlier[10] achieved similar conversions but far lower C_2H_4 selectivities at 950 °C. Note, however, that lower CH_4/S ratios and lower WHSVs were used in those experiments.[10]

It has been observed previously that CH_4 coupling to C_2 products may occur non-oxidatively at high temperatures, resulting in H_2 evolution.[9a,16] For analyzing whether this non-oxidative reaction pathway is relevant under SOCM conditions, the extent of the conversion to H_2S was investigated. Table 1

Table 1. H_2S Selectivity for Contact Times of 0.785, 0.628, and 0.471 h^{-1} and Fraction of Unreacted H_2S after Reaction at 950 °C with WHSV = 0.628 h^{-1}

	S_{H_2S} (%)			
	at 0.785 h^{-1}	at 0.628 h^{-1}	at 0.471 h^{-1}	unreacted H_2S at 0.628 h^{-1} (%)
ZnO	57.5	57.8	58.6	62.3
WO_3	−6.0	−4.4	3.2	39.3
La_2O_3	24.2	38.2	68.3	42.4
Cr_2O_3	30.0	17.5	18.3	38.0
Fe_3O_4	28.3	26.2	26	58.9

gives the ratio between the measured H_2S concentration and the H_2S concentration that would be obtained if only oxidation to C_2, CS_2, and H_2S occurred. This ratio is termed H_2S selectivity in the following discussion. Table 1 shows that the H_2S selectivity is far lower than 100% for all catalysts. On ZnO and Fe_3O_4, no strong dependence of the H_2S selectivity on the WHSV is observed, while for La_2O_3 the H_2S selectivity increases and for Cr_2O_3 it decreases with falling WHSV. On WO_3, a negative H_2S selectivity is observed at the two lower WHSVs. Accordingly, no H_2S products are formed on WO_3 catalysts, and the trace of H_2S added to the reaction mixture is consumed to some extent.

The observed low H_2S selectivities could in principle result from either the conversion of product H_2S to H_2 and S_2 or the reaction of CH_4 via a non-oxidative pathway (resulting in H_2 evolution). The former reaction pathway was probed by directing H_2S at 950 °C over the catalysts for several hours until the H_2S conversions were stable. Since the highest possible H_2S concentrations during SOCM are in the range 0.25−0.33%, a feed mixture of 0.33% H_2S in argon was used in these experiments. Column 5 of Table 1 shows that H_2S conversion to H_2 and S_2 occurs to a large extent over all catalysts, but only over ZnO and La_2O_3 is the fraction of unreacted H_2S in quantitative agreement with the H_2S selectivities at SOCM conditions for WHSV = 0.628 h^{-1}. According to the significantly lower H_2S selectivities on WO_3, Cr_2O_3, and Fe_3O_4 under SOCM conditions, non-oxidative coupling occurs over these catalysts to a significant extent.

A further question regarding the SOCM reaction pathway is whether C_2H_4 and C_2H_2 are formed via CH_2 and CH coupling, respectively, or via dehydrogenation of C_2H_6 and C_2H_4, respectively. Evidence is found from a comparison of the C_2H_6/C_2H_4 and C_2H_2/C_2H_4 ratios at different contact times, which is given in Figure 4 for selected catalysts (see SI for data on all oxides). For the oxides shown, the C_2H_6/C_2H_4 ratio decreases by 13% and 21% upon decreasing the WHSV from 0.785 to 0.628 h^{-1} and further to 0.471 h^{-1}, whereas the C_2H_2/C_2H_4 ratio increases by 16% and 10%. The relative decrease in the C_2H_6 selectivity with increasing contact time provides

DOI: 10.1021/jacs.5b09939
J. Am. Chem. Soc. 2015, 137, 15234−15240

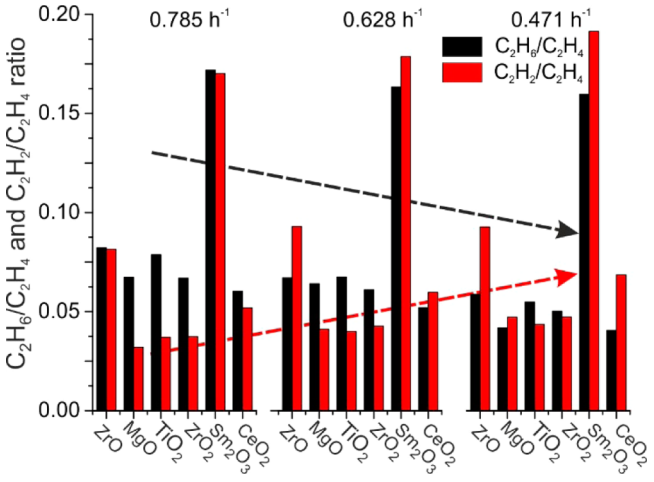

Figure 4. WHSV dependence of average C_2H_6/C_2H_4 ratios (black), and average C_2H_2/C_2H_4 ratios (red) for SOCM over selected catalysts.

strong evidence that C_2H_6 is the major source of C_2H_4. The decreasing C_2H_2/C_2H_4 ratio with decreasing WHSV further suggests that C_2H_2 is formed via C_2H_4 dehydrogenation. As on WO_3, La_2O_3, Cr_2O_3, and Fe_3O_4, a small increase in C_2H_2/C_2H_4 with contact time is detected, acetylene may be formed via another reaction pathway on these oxides. For all 10 of the present oxides, the relative CS_2 vs the C_2 content is highest at the lowest WHSV, which is expected since CS_2 is the final oxidation product.

In order to determine whether there is a relationship between the catalytic properties and the catalyst structural/compositional evolution, several analytical techniques were employed on the chalcogenides after SOCM reaction. Initially, the oxides are in the form of nanopowders with BET surface areas of ≥10 m^2/g, except for WO_3 which has a surface area of 9.3 m^2/g. As shown in Table 2, the surface areas are significantly reduced after SOCM at 950 °C, similar to previous observations on OCM with O_2.[2c,11,17] The surface areas of ZrO_2, MgO, WO_3, and La_2O_3 are >1.5 m^2/g, while the surface areas of the other oxides are smaller than 1 m^2/g.

Table 2. Structural Characteristics of Catalysts after Reaction under SOCM Catalytic Conditions at 950 °C for 16 h

	phases detected by XRD	molar S/O ratio[a]	carbon (%)[b]	surface area (m^2/g)[c]
MgO	MgS, MgO	5.66	>80	9.47
ZrO_2	ZrO_2, ZrS_2	0.07	>80	6.29
TiO_2	TiO_2, Ti_3S_4	0.05	~15	0.42
CeO_2	$Ce_{10}S_{14}O$, Ce_4S_3O	0.14	~68	0.46
Sm_2O_3	$Sm_{10}S_{14}O$, Sm_2O_2S	3.39	>80	0.18
Fe_3O_4	FeS_2, FeS, $Fe_{1-x}S$	>100	~12	0.07
ZnO	ZnS, ZnO	33.11	~36	0.22
WO_3	WS_2	9.61	>80	1.88
La_2O_3	$La_{10}S_{14}O_{0.5}$	20.82	>80	1.89
Cr_2O_3	$Cr_{1.89}S_3$, Cr_2S_3	4.75	~10	0.67

[a]S/O ratio by combustion analysis. [b]C content by XPS. [c]BET surface area in m^2/g.

X-ray diffraction analysis shows that the spent catalysts generally consist of metal sulfides, oxides, and oxysulfides.[18] Note that Table 2 only shows unambiguously identified phases in the order of the intensity of their respective Bragg peaks. This does not exclude the presence of further crystalline phases, present in lower concentrations. The high intensities of the Bragg peaks for the Mg and Zn chalcogenides suggest that they are highly crystalline. The significantly less pronounced reflections for Ce, Sm, and La chalcogenides provides evidence that they are amorphous to a large extent. On the oxides of Mg, Zr, Ti, Fe, Zn, and W after reaction, crystalline sulfides and oxides are observed, whereas mixed phases are detected on the other chalcogenides.

The extent of oxide → sulfide conversion is strongly oxide dependent. On the basis of the sulfur and carbon content, obtained from combustion analysis, and the major crystalline phases, detected by XRD, the molar S/O content of the chalcogenides was estimated and is shown in Table 2. The high S/O ratios for the Mg, Sm, Zn, W, La, and Cr chalcogenides show that they contain significantly more S than O, while the Fe_3O_4 is almost entirely converted to a sulfide. In contrast, the Zr, Ti, and Ce catalysts largely consist of oxides after SOCM.

XPS was also employed to study the surface properties of the present catalysts after reaction. Table 2 shows that the major fraction of the Mg, Zr, Sm, W, and La catalyst surfaces is covered with a carbonaceous species. In agreement with these results, data from combustion analysis show that >0.5 wt% of carbon is present on these substrates. Note that this level of coking was not observed previously for the Pd-based SOCM catalysts.[6] In contrast, only minor carbonaceous species are observed on the Cr, Zn, Fe, and Ti catalysts with the coke surface content of CeO_2 after reaction being ~68%. The nature of the carbonaceous species was also investigated by UV Raman spectroscopy on selected catalysts. On the Mg, Zr, and Sm chalcogenides, Raman bands at ~1600 and ~1350 cm^{-1} are detected, which are the characteristic bands for graphite and defective/amorphous carbon ("coke").[12] Both features are significantly weaker on CeS_xO_y and are absent on the Ti and Fe catalysts (spectra shown in the SI).

The spent Ti, Fe, Zn, and Cr SOCM catalysts not only have a significantly lower surface carbon content, but also differ from the other catalysts in the nature of the surface O species. On these chalcogenides, XPS O 1s features at 530−531 eV are assignable to neat metal oxides,[13] whereas negligible or only very weak features in this region are observed on the Mg, Ce, Sm, and Zr catalysts (SI). Although all catalysts exhibit a peak at ~532 eV, this feature decays in intensity upon sputtering on the catalysts that form only minor amounts of coke. Accordingly, this peak may result from surface H_2O or OH. For the coked catalysts on which no strong decay of the 532 eV peak is observed, the presence of a C−O−C species is suggested.[19] On both types of catalysts, S 2p transitions at 161−162 eV confirm the presence of metal sulfides.[20,21] The spent Sm, Ce, Zr, Mg, La, and W catalysts, which contain considerable amounts of surface coke also exhibit a doublet at ~164 eV which is assignable to C−S−C, or S_n species.[19]

For all of the above catalysts, sputtering for 30 s with 30 keV Ar^+ ions does not significantly attenuate the XPS S 2p peaks, indicating the sulfur concentration only insignificantly changes to a depth of several nm. Similarly, the C 1s signal on the coked catalysts does not strongly change on 30 s Ar^+ sputtering. This is not the case for the Fe, Ti, Zn, and Cr, catalysts which only coke to a minor extent, suggesting that the corresponding carbonaceous species are predominantly adventitious surface carbon.

DOI: 10.1021/jacs.5b09939
J. Am. Chem. Soc. 2015, 137, 15234−15240

DISCUSSION

Figure 5 presents a tentative structural model for the two types of chalcogenide catalysts discussed here. Generally, a mixture of

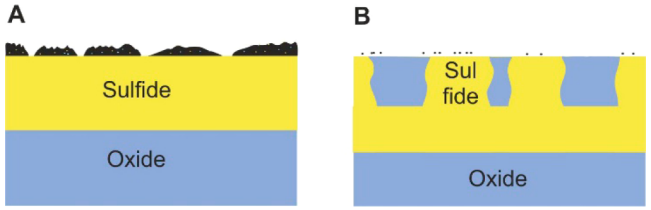

Figure 5. Schematic representation of the two different types of surfaces formed during SOCM at 950 °C.

oxides and sulfides is present after SOCM. On type A catalysts, based on MgO, Sm_2O_3, ZrO_2, La_2O_3, and WO_3, after reaction, significant amounts of coke containing O and S are found. Beneath the coke layer, a metal sulfide forms during SOCM. On type B catalysts, based on Ti, Fe, Zn, and Cr oxides, only minor surface C is present in addition to an oxide and a sulfide. Note that Figure 5 is somewhat ambiguous in that the sulfide/oxide content is strongly catalyst dependent; as seen from Table 2, the S/O ratio in the catalyst ranges from 0.05 to >100. In principle, the extent of oxide → sulfide conversion should depend mainly on cation and anion diffusion in the solid state, and the reactivity of the catalyst surface with S_2.[22]

In previous OCM studies, coking was not observed due to the presence of the strong oxidant O_2. In contrast, coke formation has been reported, e.g., in non-oxidative CH_4 coupling, hydrocarbon pyrolysis, and CH_4 steam reforming.[16d,e,23] It was observed in those studies that coking usually leads to a gradual deactivation of the catalyst.[9h,21,24] In contrast, no deactivation has been observed in the present work. Although for some of the coke-forming catalysts, CH_4 conversion drops while the C_2H_4 selectivity increases during first few hours, the catalytic properties are subsequently stable for a number of hours. Even after adjusting the WHSV from 0.785 to 0.628 h^{-1}, and 5 h later to 0.471 h^{-1}, no consistent decline in CH_4 conversion is observed. Since CH_4 diffusion on the surfaces before reaction should be negligible, it is concluded that CH_4 is readily activated on the coked surfaces.

As discussed above, the high S_2 conversions lead to a small range of CH_4 conversions, which is most pronounced for the lowest WHSV at which the S_2 conversion is highest. In contrast, the C_2H_4 selectivity is strongly catalyst dependent as shown in Figure 2 a (WHSV = 0.785 h^{-1}). To determine whether catalysts that coke have distinctly different catalytic properties from catalysts that do not coke, CH_4 conversion and C_2H_4 selectivities on the former and latter are compared. On average, the CH_4 conversion is 33% lower on the non-coking catalysts, whereas the C_2H_4 selectivities are 69% higher. In fact, none of the four catalysts on which measured C_2H_4 selectivities are larger than 25% (Zn, Cr, Fe, Ce) contain >80% surface carbon after reaction. It can be speculated whether these catalysts have sites with enhanced reactivities that readily activate CH_4 intermediates to form coke or whether there are simply a larger number of reaction sites leading to coke formation. The latter hypothesis would be supported by the enhanced surface areas of four of the five catalysts that strongly coke (>80% surface C).

Having established that strongly coking catalysts give low C_2H_4 selectivities and yields, the question next arises as to which intrinsic metal properties favor high ethylene yields. Since several oxidation states are accessible to Cr, Fe, and Ce, it might be concluded that more redox-active metals are necessary for obtaining enhanced C_2H_4 selectivities. However, the Zn chalcogenide is also found to be highly selective although the only stable Zn oxidation state is +2. To reliably establish, which intrinsic properties of the chalcogenides favor high C_2H_2 selectivities, in-depth studies on the adsorption properties and catalyst electronic structure will be necessary, which are beyond the scope of this work. It is noteworthy that for SOCM, transition metal oxides were found to show high selectivities to ethylene. In contrast, numerous OCM studies on single metal oxides revealed that predominantly alkaline earth oxides and rare earth oxides give high C_2 selectivities.[3b] This trend highlights a fundamental difference between OCM and SOCM catalytic characteristics.

Regarding the SOCM reaction pathway, a homolytic cleavage of CH_4 to form CH_3 is reasonably expected to be the initial step as in OCM and non-oxidative CH_4 coupling.[2d,g,3a,f,9a,16d,25] C_2H_4 may then be formed via CH_3 coupling to C_2H_6 and subsequent dehydrogenation, or CH_2 formation and subsequent coupling to C_2H_4. Previous OCM studies mostly agree that C_2H_4 is predominantly formed via C_2H_6 dehydrogenation,[2d,3f,26] whereas DFT studies on neat metal sulfides find that C_2H_4 is likely formed via CH_2 coupling in SOCM.[10] The present findings that the relative C_2H_6 selectivity with respect to the C_2H_4 selectivity decreases with increasing contact time provides strong evidence that C_2H_4 is formed via C_2H_6 dehydrogenation. Likewise, C_2H_2 may be formed via C_2H_4 dehydrogenation and/or CH coupling. In previous mechanistic studies on non-oxidative CH_4 coupling, C_2H_2 formation via dehydrogenation of ethylene was found/assumed.[16d] In the present work, increasing contact times lead to a relative increase in the C_2H_2 selectivity with respect to the C_2H_4 selectivity for the catalysts shown in Figure 4. Accordingly, C_2H_2 formation via C_2H_4 is anticipated in these cases. For the W, Cr, La, and Fe catalysts, however, a relative decrease in the C_2H_2 selectivity with increasing contact time is observed, suggesting that other pathways for acetylene formation may predominate. That the relative CS_2 selectivity with respect to the C_2 selectivity is highest for the highest contact time is expected since CS_2 is the final oxidation product. CS_2 may be formed by dehydrogenation of C_2H_2 or surface CH_x, possibly via further intermediates.

In depth mechanistic studies on CH_4 pyrolysis revealed that acetylene is a key intermediate species for coke formation.[16d,23a,27] Upon examining the present C_2H_2/C_2H_4 ratios at the lowest WHSV at which coke formation is expected to be most prominent, it is found that Fe_3O_4, Cr_2O_3, and TiO_2, which do not coke show the lowest C_2H_2/C_2H_4 ratios (SI). That a low C_2H_2 selectivity correlates with suppressed coke formation suggests that in SOCM, coke deposition occurs via C_2H_2, agreeing with previous studies.

Compared to our previous SOCM study, enhanced C_2H_4 selectivities of up to 33% have been obtained at similar conversions (5−12%). Of course, these values are currently below commercial interest and significantly higher C_2 yields were found previously in OCM studies. Note however that the desired reaction product C_2H_4 is by far the most prominent C_2 product in SOCM: the C_2H_4/C_2H_6 ratio is 8.9−12.4 (WHSV = 0.471 h^{-1}), which is to our knowledge higher than in any

DOI: 10.1021/jacs.5b09939
J. Am. Chem. Soc. 2015, 137, 15234−15240

previous OCM study in which the relative selectivities toward C_2H_4 and C_2H_6 were reported. Second, oxidative coupling of CH_4 with S_2 has barely been explored, and further studies on optimizing the catalysts and reaction conditions are likely to provide higher ethylene yields.

CONCLUSIONS

The goal of the present investigation was to explore OCM processes over a series of metal oxides with S_2 as the oxidant. Substantially greater C_2H_4 selectivities are found versus previous SOCM work, and significantly higher C_2H_4/C_2H_6 ratios are achieved than previously reported for OCM with O_2. No deactivation on Fe_3O_4 is found over 48 h of SOCM with the other catalysts also exhibiting stable catalytic properties for 16 h on-stream.

While the present Mg, Zr, Sm, W, and La catalysts form significant amounts of coke during SOCM, only minor coking takes place over Fe, Ti, and Cr catalysts. The extent of the sulfur conversion and presence of oxides on the surface are strongly catalyst dependent. That C_2H_4 selectivities of >25% are only found on non-coking catalysts suggests that some degree of coking resistance facilitates optimum CH_4 conversions to C_2 products.

The relative C_2H_6, C_2H_4, and C_2H_2 selectivities as a function of WHSV provide evidence for the formation of C_2H_4 and C_2H_2 via dehydrogenation of C_2H_6 and C_2H_4, respectively. Catalyst-dependent, non-oxidative CH_4 coupling is also relevant. Further studies of SOCM scope and mechanism are in progress.

ASSOCIATED CONTENT

Supporting Information

The Supporting Information is available free of charge on the ACS Publications website at DOI: 10.1021/jacs.5b09939.

Details of reactor measurements, and Raman, XRD, and XPS spectra (PDF)

AUTHOR INFORMATION

Corresponding Author

*t-marks@northwestern.edu

Notes

The authors declare no competing financial interest.

ACKNOWLEDGMENTS

We thank the Dow Chemical Co. for support of this research as part of the Methane Challenge. M.P. thanks DFG for a postoctoral fellowship with reference number PE 2321/1-1. This work made use of the J.B.Cohen X-ray Diffraction Facility at the Materials Research Center of Northwestern University. XPS and Raman experiments were performed in the Keck-II facility of the NUANCE Center at Northwestern University. We thank Dr. M. Delferro for helpful suggestions.

REFERENCES

(1) (a) Basic Energy Sciences Advisory Committee. *Directing Matter and Energy: Five Challenges for Science and the Imagination*; U.S. Department of Energy, National Academy Press, 2007. (b) ICIS Home Page, Indicative Chemical Prices, http://www.icis.com/chemicals/channel-info-chemicals-a-z/ (accessed Feb 12, 2015).

(2) (a) Keller, G. E.; Bhasin, M. M. *J. Catal.* **1982**, *73*, 9−19. (b) Ito, T.; Wang, J. X.; Lin, C.; Lunsford, J. H. *J. Am. Chem. Soc.* **1985**, *107*, 5062−5068. (c) Campbell, K. D.; Morales, E.; Lunsford, J. H. *J. Am. Chem. Soc.* **1987**, *109*, 7900−7901. (d) Lee, J. S.; Oyama, S. T. *Catal. Rev.: Sci. Eng.* **1988**, *30*, 249−280. (e) Peil, K. P., Jr.; Goodwin, J. G.; Marcelin, G. *J. Am. Chem. Soc.* **1990**, *112*, 6129−6130. (f) Weng, W.; Chen, M.; Wan, H.; Liao, Y. *Catal. Lett.* **1998**, *53*, 43−50. (g) Mallens, W. P. J.; Hoebink, J. H. B. J.; Marin, G. B. *J. Catal.* **1996**, *160*, 222−234. (h) Myrach, P.; Nilius, N.; Levchenko, S. V.; Gonchar, A.; Risse, T.; Dinse, K.-P.; Boatner, L. G.; Frandsen, W.; Horn, R.; Freund, H.-J.; et al. *ChemCatChem* **2010**, *2*, 854−862. (i) Yildiz, M.; Simon, U.; Otremba, T.; Aksu, Y.; Kailasam, K.; Thomas, A.; Schomäcker, R.; Arndt, S. *Catal. Today* **2014**, *228*, 5−14.

(3) (a) Lunsford, J. H. *Angew. Chem., Int. Ed. Engl.* **1995**, *34*, 970−980. (b) Zavyalova, U.; Holena, M.; Schlögl, R.; Bärns, M. *ChemCatChem* **2011**, *3*, 1935−1947. (c) Beck, B.; Fleischer, V.; Arndt, S.; Hevia, M. G.; Urakawa, A.; Hugo, P.; Schomäcker, R. *Catal. Today* **2014**, *228*, 212−218. (d) Simon, U.; Görke, O.; Berthold, A.; Arndt, S.; Schomäcker, R.; Schubert, H. *Chem. Eng. J.* **2011**, *168*, 1352−1359. (e) Arndt, S.; Laugel, G.; Levchenko, S.; Horn, R.; Baerns, M.; Scheffler, M.; Schlögl, R.; Schomäcker, R. *Catal. Rev.: Sci. Eng.* **2011**, *53*, 424−514. (f) Takanabe, K.; Iglesia, E. *J. Phys. Chem. C* **2009**, *113*, 10131−10145.

(4) (a) Bullis, K. *MIT Technology Review*, Jan 18, 2014. (b) Siluria Technologies, http://siluria.com (accessed July 16, 2015).

(5) (a) Arndt, S.; Otremba, T.; Simon, U.; Yildiz, M.; Schubert, H.; Schomäcker, R. *Appl. Catal., A* **2012**, *425−426*, 53−61. (b) Da, J.; Ding, X.; Shen, S. *Appl. Catal., A* **1994**, *116*, 81−94. (c) Xu, Y.; Yu, L.; Cai, C.; Huang, J.; Guo, X. *Catal. Lett.* **1995**, *35*, 215−231. (d) Olivier, L.; Haag, S.; Pennemann, H.; Hofmann, C.; Mirodatos, C.; Van Veen, A. C. *Catal. Today* **2008**, *137*, 80−89. (e) Lomonosov, V.; Gordienko, Z.; Sinev, M. *Top. Catal.* **2013**, *56*, 1858−1866.

(6) Arndt, S.; Laugel, G.; Levchenko, S.; Horn, R.; Baerns, M.; Scheffler, M.; Schlögl, R.; Schomäcker, R. *Catal. Rev.: Sci. Eng.* **2011**, *53*, 424−514.

(7) (a) Egorov, S. A.; Bobrova, S. F.; Bondar, A. D.; Shcherbakov, P. M. *Gazovaya Promyshlennost* **1986**. (b) Hunter, N. R.; Gesser, H. D.; Morton, L. A.; Yarlagadda, P. S.; Fung, D. P. C. *Appl. Catal.* **1990**, *57*, 45−54. (c) Labinger, J. A. *J. Mol. Catal. A: Chem.* **2004**, *220*, 27−35.

(8) (a) Ohtsuka, K. *Petrotech* **1995**, *18*, 826−870. (b) Shi, C.; Sun, Q.; Hu, H.; Herman, R. G.; Klier, K.; Wachs, I. E. *Chem. Commun.* **1996**, *5*, 663−664. (c) de Vekki, A. V.; Marakaev, S. T. *Russ. J. Appl. Chem.* **2009**, *82*, 521−536. (d) Wang, Z.-C.; Dietl, N.; Kretschmer, R.; Ma, J.-B.; Weiske, T.; Schlangen, M.; Schwarz, H. *Angew. Chem., Int. Ed.* **2012**, *51*, 3703−3707.

(9) (a) Borry, R. W.; Lu, E. C.; Kim, Y.-H.; Iglesia, E. *Stud. Surf. Sci. Catal.* **1998**, *119*, 403−410. (b) Hamakawa, S.; Hibino, T.; Iwahara, H. *J. Electrochem. Soc.* **1993**, *140*, 459−462. (c) Langguth, J.; Dittmeyer, R.; Hoffmann, H.; Tomandl, G. *Appl. Catal., A* **1997**, *158*, 287−305. (d) Chen, L.; Lin, L.; Xu, Z.; Zhang, T.; Li, X. *Catal. Lett.* **1996**, *39*, 169−172. (e) Zhang, J.-Q.; Yang, Y.-J.; Zhang, J.-S.; Liu, Q.; Tan, K.-R. *Energy Fuels* **2002**, *16*, 687−693. (f) Soulivong, D.; Norsic, S.; Taoufik, M.; Coperet, C.; Thivolle-Cazat, J.; Chakka, S.; Basset, J.-M. *J. Am. Chem. Soc.* **2008**, *130*, 5044−5045. (g) Jiang, H.; Cao, Z.; Schirrmeister, S.; Schiestel, T.; Caro, J. *Angew. Chem., Int. Ed.* **2010**, *49* (33), 5656−5660. (h) Cao, Z.; Jiang, H.; Luo, H.; Baumann, S.; Meulenberg, W. A.; Assmann, J.; Mleczko, L.; Liu, Y.; Caro, J. *Angew. Chem., Int. Ed.* **2013**, *52* (51), 13794−7. (i) Nemana, S.; Gates, B. C. *Catal. Lett.* **2007**, *113*, 73−81. (j) Guo, X. G.; Fang, G. Z.; Li, G.; Ma, H.; Fan, H. J.; Yu, L.; Ma, C.; Wu, X.; Deng, D. H.; Wei, M. M.; Tan, D. L.; Si, R.; Zhang, S.; Li, J. Q.; Sun, L. T.; Tang, Z. C.; Pan, X. L.; Bao, X. H. *Science* **2014**, *344*, 616−619. (k) Khan, M.; Crynes, B. *Ind. Eng. Chem.* **1970**, *62*, 54−59.

(10) Zhu, Q.; Wegener, S. L.; Xie, C.; Uche, O.; Neurock, M.; Marks, T. J. *Nat. Chem.* **2012**, *5* (2), 104−109.

(11) Jüngst, E.; Nehb, W. *Handbook of Heterogeneous Catalysis*; Wiley-VCH: Weinheim, 2008; Chapter 12.4.

(12) (a) Farbenindustrie, I. German Patent GB293172, 1927. (b) Simo, M. U.S. Patent US2187393, 1940. (c) Thacker, C. M. U.S. Patent US2330934, 1943. (d) Plier, M.; Winkler, K. U.S. Patent US1735409, 1929. (e) Preda, M. Belgian Patent BE630584, 1963. (f) Bodenstein, P. H. U.S. Patent US1981161, 1984.

DOI: 10.1021/jacs.5b09939
J. Am. Chem. Soc. 2015, 137, 15234−15240

(13) (a) Anderson, J. R.; Chang, Y.-F.; Pratt, K. C.; Foger, K. *React. Kinet. Catal. Lett.* **1993**, *49*, 261−269. (b) Karan, K.; Behie, L. A. *Ind. Eng. Chem. Res.* **2004**, *43*, 3304−3313.
(14) Didenko, L. P.; Linde, V. R.; Savchenko, V. I. *Catal. Today* **1998**, *42*, 367−370.
(15) (a) Dubois, J.-L.; Rebours, B.; Cameron, C. J. *Appl. Catal.* **1990**, *67*, 73−79. (b) Tong, Y.; Rosynek, M. P.; Lunsford, J. H. *J. Catal.* **1990**, *126*, 291−298. (c) Otsuka, K.; Jinno, K.; Morikawa, A. *Chem. Lett.* **1985**, *14*, 499−500. (d) Dubois, J.-L.; Cameron, C. J. *Appl. Catal.* **1990**, *67*, 49−71. (e) Rezgui, S.; Liang, A.; Cheung, T.-K.; Gates, B. C. *Catal. Lett.* **1998**, *53*, 1−2.
(16) (a) Gordon, A. S. *J. Am. Chem. Soc.* **1948**, *70*, 395−401. (b) Palmer, H.; Lahaye, J.; Hou, K. *J. Phys. Chem.* **1968**, *72*, 348−353. (c) Billaud, F. G.; Baronnet, F.; Gueret, C. P. *Ind. Eng. Chem. Res.* **1993**, *32*, 1549−1554. (d) Holmen, A.; Olsvik, O.; Rokstad, O. A. *Fuel Process. Technol.* **1995**, *42*, 249−267. (e) Li, L.; Borry, R. W.; Iglesia, E. *Chem. Eng. Sci.* **2002**, *57*, 4595−4604.
(17) (a) Au, C. T.; He, H.; Lai, S. Y.; Ng, C. F. *Appl. Catal., A* **1997**, *159*, 133−145. (b) Mahmoodi, S.; Ehsani, M. R.; Ghoreishi, S. M. *J. Ind. Eng. Chem.* **2010**, *16*, 923−928.
(18) ICDD. *PDF-4+ 2014*; Kabekkodu, S., Ed.; International Centre for Diffraction Data: Newton Square, PA, USA, 2014.
(19) Beamson, G.; Briggs, D., *The Scienta ESCA300 Database*; Wiley Interscience: New York, 1992.
(20) (a) Franzen, H. F.; Umana, M. X.; McCreary, J. R.; Thorn, R. J. *J. Solid State Chem.* **1976**, *18*, 363. (b) Gonbeau, D.; Guimon, C.; Pfister-Guillouzo, G.; Levasseur, A.; Meunier, G.; Dormoy, R. *Surf. Sci.* **1991**, *254*, 81−89. (c) Pratt, A. R.; Muir, J. J.; Nesbitt, H. W. *Geochim. Cosmochim. Acta* **1994**, *58*, 827−841. (d) Hernan, L.; Morales, J.; Sanchez, L.; Tirado, J. L.; Espinos, J. P.; Gonzalez Elipe, A. R. *Chem. Mater.* **1995**, *7*, 1576. (e) Moreau, P.; Ouvrard, G.; Gressier, P.; Ganal, P.; Rouxel, J. *J. Phys. Chem. Solids* **1996**, *57*, 1117. (f) Nesbitt, H. W.; Bancroft, G. M.; Pratt, A. R.; Scaini, M. J. *Am. Mineral.* **1998**, *83*, 1067−1076. (g) Baltrusaitis, J.; Jayaweera, P. M.; Grassian, V. H. *J. Phys. Chem. C* **2011**, *115*, 492−500.
(21) (a) Kim, H. S.; Arthur, T. S.; Allred, G. D.; Zajicek, J.; Newman, J. G.; Rodnyansky, A. E.; Oliver, A. G.; Boggess, W. C.; Muldoon, J. *Nat. Commun.* **2011**, *2*, 427. (b) Wang, X.-F.; Xiong, S.-M. *Metall. Mater. Trans. A* **2012**, *43* (11), 4406−4413. (c) Overbury, S. H.; Mullins, D. R.; Huntley, D. R.; Kundakovic, L. *J. Phys. Chem. B* **1999**, *103*, 11308−11317. (d) Smirnov, M. Y.; Kalinkin, A. V.; Pashis, A. V.; Sorokin, A. M.; Noskov, A. S.; Bukhtiyarov, V. I.; Kharas, K. C.; Rodkin, M. A. *Kinet. Catal.* **2003**, *44*, 575−583. (e) Ferrizz, R. M.; Gorte, R. J.; Vohs, J. M. *Catal. Lett.* **2002**, *82*, 123−129. (f) Wong, P. C.; Li, Y. S.; Zhou, M. Y.; Mitchell, K. A. R. *Surf. Rev. Lett.* **1995**, *2*, 165−169.
(22) (a) Mizusaki, J. *Gen. Rev.* **1989**, *31*, 33−227. (b) Ovsitser, O. Y.; Sokolovskii, V. D. *Catal. Lett.* **1993**, *17*, 239−244. (c) Grabke, H. J. *Defect Diffus. Forum* **2001**, *194*−*199*, 1649−1660. (d) Ikuma, Y.; Kamiya, M.; Shimada, E. *Key Eng. Mater.* **2003**, *253*, 225−242. (e) Nowotny, J.; Bak, T.; Nowotny, M. K.; Sheppard, L. R. *Ionics* **2006**, *12*, 227−243. (f) Chevalier, S. *Defect Diffus. Forum* **2009**, *289*−*292*, 405−412.
(23) (a) Gascoin, N.; Gillard, P.; Bernard, S.; Bouchez, M. *Fuel Process. Technol.* **2008**, *89*, 1416−1428. (b) Gascoin, N.; Abraham, G.; Gillard, P.; Bouchez, M. *J. Anal. Appl. Pyrolysis* **2011**, *91*, 377−387. (c) Cruzan, A.; Palmer, G. H. US 2618542, 1952;.
(24) (a) Henriques, C.; Guisnet, M. *Gen. Rev.* **2011**, *9*, 253−267. (b) Trimm, D. L. *Chem. Eng. Process.* **1984**, *18*, 137−48. (c) Twigg, M. V.; Spencer, M. S. *Top. Catal.* **2003**, *22*, 191−203.
(25) Roos, J. A.; Korf, S. J.; Veehof, R. H. J.; van Ommen, J. G.; Ross, J. R. H. *Appl. Catal.* **1989**, *52*, 131−145.
(26) (a) Palermo, A.; Holgado Vazquez, J. P.; Lee, A. F.; Tikhov, M. S.; Lambert, R. M. *J. Catal.* **1998**, *177*, 259−266. (b) Zohour, B.; Noon, D.; Senkan, S. *ChemCatChem* **2013**, *5*, 2809−2812. (c) Chen, C.; Back, M.; Back, R. *Can. J. Chem.* **1975**, *53*, 3580−3590.
(27) (a) Lahaye, J.; Prado, G. *ACS Symp. Ser.* **1976**, *21*, 335−349. (b) Frenklach, M.; Wang, H. *Symp. Combust., [Proc.]* **1991**, *23*, 1559−1566. (c) Fau, G.; Gascoin, N.; Gillard, P.; Steelant, J. *J. Anal. Appl. Pyrolysis* **2013**, *104*, 1−9.

DOI: 10.1021/jacs.5b09939
J. Am. Chem. Soc. 2015, 137, 15234−15240